EVALUATION OF THERMO-ELASTIC STRESS ANALYSIS (TSA) AND DIGITAL IMAGE CORRELATION (DIC) TECHNIQUES FOR DETECTION OF DELAMINATION CRACK PROPAGATION OF GLASS EPOXY COMPOSITE PLATE UNDER UNI-AXIAL CYCLIC LOADING

Ayad Kakei [b,c], J.A. Epaarachchi [a], Mainul Islam [a], J. Leng [c,d], Anura P. Rathnayake[e] , N.K. Hettiarachchi[e]

[a] Centre of Future Materials, University of Southern Queensland, West Street, Toowoomba, QLD 4350, Australia
[b] University of Kirkuk, College of Engineering, Kirkuk, Iraq
[c] School of Mechanical & Electrical Engineering & Centre of Excellence in Engineered Fibre Composites, University of Southern Queensland, West Street, Toowoomba, QLD 4350, Australia
[d] Centre for Smart Materials and Structures, School of Astronautics, Harbin Institute of Technology, Harbin 150001, China
[e] Department of Mechanical and manufacturing Engineering, University of Ruhuna, Hapugala, Galle 80000 Sri Lanka

ABSTRACT

Delamination is the most common failures in composite structures and has harmful effects on the structure integrity. As such, a proper monitoring system of delamination crack propagation is an urgent need for advanced composites structures in various engineering applications. This paper details an investigation performed on the use of Thermal Stress Analysis (TSA) and Digital Image Correlation (DIC) Techniques to monitor delamination crack propagation in a glass fibre reinforced composite sample. Also a finite element analysis using cohesive elements to simulate delamination crack propagation has performed. It has been found that TSA techniques have performed well for monitoring delamination crack. The DIC techniques showed a significant influence of the location of the crack through the thickness direction on its sensitivity. Further FEA results have shown a good correlation with the experimental results.

Keywords: Structural health monitoring, TSA, DIC technique, Delamination, Composite materials

1. INTRODUCTION

Delamination between plies of a laminate is one of the critical and dangerous failure modes of GFRP because it significantly reduces the inter-laminar strength between the neighbouring fibre and matrix. The growth of delamination leads to a rapid decline of the mechanical properties of GFRP which would cause catastrophic failures of GFRP composite components [12, 13]. The delamination is a hidden killer of many FRP composite components and has been a widely researched area in FRP material development field. Although insight to the delamination process has been theoretically modelled by various researchers [7, 8, 10, 11, 14, 15], unfortunately none of the developed models were able to accurately predict the delamination process of wider range of GFRP material. Thus more robust model is needed for prediction of delamination process accurately.

Non-destructive TSA method has shown a capability to estimate damage in composite structures. Many recent studies have shown that the TSA based techniques are powerful tools for estimating damage in fibre reinforced polymeric materials. A study was carried out on a damage in a single lap joint using TSA and correlated to microstructural analysis in carbon fiber/epoxy composite[5]. This study has proved the ability of TSA method to capture early stages of damage in bonded joints. However, the investigation of the delamination by TSA is remaining as a relatively narrow research field of activity and extended studies are warranted to find robust techniques to use for a wider range of FRP materials. .

Non-contact optical methods for investigating damage accumulation and propagation in composite materials include both interferometric techniques and non-interferometric techniques. The interferometric methods require the special and high sensitive methodologies and techniques such as a coherent light source, a vibration isolated optical platform, and a powerful fringe processing such as Holographic Non-Destructive Testing (HNDT) method , Electronic Speckle Pattern Interferometry (ESPI) technique and a phase analysis techniques to measure the phase difference of the scattered light wave from the test object surface [1]. The Non- interferometric techniques such as the grid method and digital image correlation (DIC) generally have less stringent requirements under experimental conditions. The DIC technology determines the deformation by comparing the grey intensity changes of the object surface before and after deformation[2]. DIC techniques have been applied to detect the deformation in the homogeneous materials and past few years DIC techniques has been successfully extended to investigate the initiation and propagation of damage in composite materials [4]. Although DIC techniques have shown significant achievements in composite material field, unfortunately some limitations and errors still remaining in the data processing algorithms. Furthermore DIC is not able to accurately measure strain near the cracks due to high strain concentration and considered as a nano-scale stress analysis method.

The Thermoelastic effect was theoretically demonstrated by William Thomson (Lord Kelvin) in 1853. A linear relationship between the temperature change of a solid and the change in the sum of principle stress for isotropic materials was presented as:

$$\frac{\Delta T}{T_0} = -K_0 \Delta\sigma \qquad (1)$$

Where, T_0 is the average temperature of the solid, $K_0=\lambda/\rho\, Cp$ is the thermoelastic constant, λ is the linear thermal expansion coefficient, ρ the mass density, Cp the specific heat at constant pressure, and $\Delta\sigma = \Delta(\sigma_1+\sigma_2+\sigma_3)$ is the variation of the first stress invariant. Recently [3] have extended this relationship for anisotropic materials as:

$$C_p \frac{\Delta T}{T_0} = -(\alpha_{11}\Delta\sigma_{11} + \alpha_{22}\Delta\sigma_{22} + \alpha_{12}\Delta\sigma_{12}) \qquad (2)$$

In order to apply this measurement principle to distinguish stress maps, it is necessary to measure a spatial distribution of temperature changes. In order to have a non-contact stress measurement technique temperature changes can be measured without contact on the surface on a loaded mechanical component by differential thermal camera. Typically temperature fluctuations are measured synchronous with a reference signal, related to the loading cycle of the mechanical component. The data processing is performed by the lock-in techniques, the mix output signal from the infrared detector with a reference signal related to the dynamic loading.

Mapping full strain field of each layer of a composite structure under various loading regimes using an experimental method will provide ultimate solution for finding damage in a composite structure [6]. However there is no available means of measuring and mapping strain field at each layer of a composite. Recent advances in full-field measurement techniques using digital image correlation (DIC) enables mapping of full strain field of the exposed surface of any composite material without having extensive strain gauge networks[9]. Further this technique eliminates the unresolved engineering

challenges associated with implementation of large sensor networks for strain mapping. Unfortunately a limited research work has been executed on DIC techniques to date due to many reasons including comparatively high cost associated with DIC infrastructure. However a few recent research work have demonstrated the significance of DIC techniques in full-field strain measurements and its extended use for investigation of damage accumulation and structural health. The accurate full field strain map provides invaluable information about structural status inside the component. These techniques are capable of identifying deformations of a surface at pixel level which is in the order less than micro meters.

This paper presents an application of Digital Image Correlation (DIC) and Thermoelastic Stress Analysis (TSA) using MITE software for detection of delamination crack propagation in glass fibre reinforced plastic (GFRP) plate. This non-destructive testing (NDT) methods which would be extremely useful in experimental fatigue life analysis of complicated composite components. In this study a FEA model has been developed with cohesive finite elements and validated with experimental results.

2. FABRICATION OF THE SPECIMEN

The material examined in the present work is a fifteen-layer (0/90) AR 145 E-glass woven roving (398 g/m^2 weight and 0.5 mm thickness) fibre-reinforced epoxy resin matrix composite that has a nominal density of 1698 kg/m3. Kenetix R246TX epoxy resin was used as the matrix material. The plain weave structure of the WC laminate consisted of two mutually orthogonal directions (warp and weft) with an approximate glass volume fraction of 60%. An artificial delaminations 50 × 40 mm^2 in size was made between the 4th–5th layers (relative to the bottom), by embedding Teflon paper (0.001 mm thickness) during manufacture. One large specimen was manufactured and then cut into smaller rectangular 400 x 40 mm^2 coupons as shown in Figure 1a. Each coupon was coated with aerosol matt black paint to produce a uniformly high surface emissivity for thermographic inspection. For DIC technique to work well a grey scale random pattern is needed on the surface of the specimen as shown in Figure 1b.

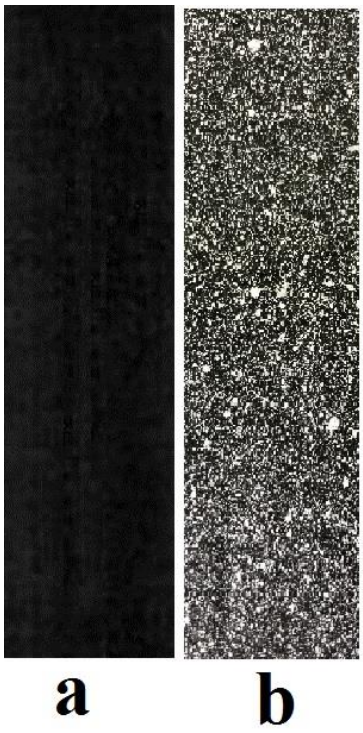

Figure 1. (a) Composite sample (TSA sample), (b) DIC sample (no hole)

3. EXPERIMENTATION

The tensile testing equipment and the test configuration is shown in Figure (2). Static and cyclic tensile loadings were applied using a constant amplitude cyclic load. The load was increased incrementally from 5kN to 35kN in steps of 5kN. Each increase in mean load was applied under displacement control at a rate of 1.5mm/min. the cyclic-load amplitude was 3kN and approximately 10000cycles were applied at each step at a frequency of 5 Hz. All tests were conducted on MTS 810, 100 kN uniaxial material testing machine fitted with hydraulic grips. The schematic of the TSA setup is shown in Figure 2. The TSA system used a FLIR A325 commercial microbolometer camera. This device contains a 320 (H) _ 240 (V) Vanadium Oxide (VOx) array with a noise equivalent temperature detectivity (NETD) of 50 mK. The camera outputs data in 16-bit digital form supplied at a fixed rate of 60 frames per second[6].

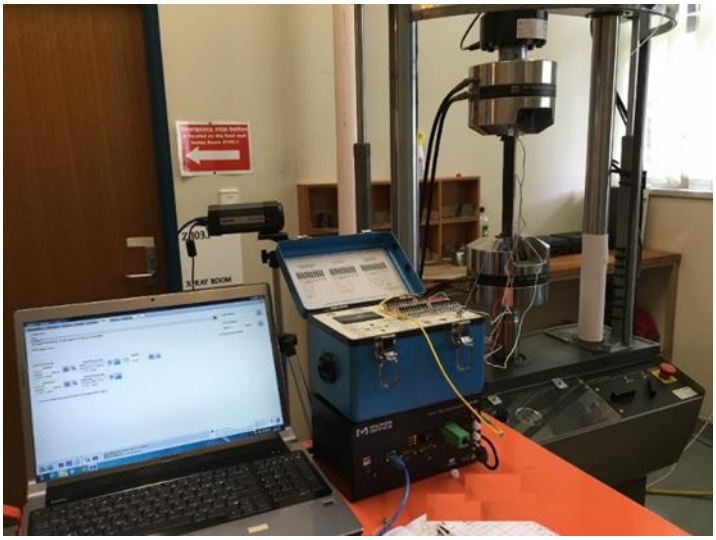

Figure 2. Experimental test setup

4. RESULT AND DISCUSSION

For comparison a detailed finite element model of the specimen was created on ABAQUS 6.13 software as shown in Figure 3. The specimen was modelled using 3D solid elements (C3D8I) with the top and bottom parts of the specimen (referring to the sections above and below the cracks) consisting of 8 layers (a thickness of 4 mm), and the middle section 6 layers (a thickness of 3.5 mm). Delamination growth was simulated using cohesive elements (COH3D8) 0.001 mm in thickness embedded at the interfaces as shown in Figure 4. The user cohesive elements technique was implemented by means of inputting a user material subroutine UMAT. Auto Desk_ Simulation composite analysis 2015 Plug-ins_ for Abaqus 6.13 were used to create the UMAT subroutine to calculate the nine state variables for the cohesive materials[6]. These state variables are stored by Abaqus at each individual integration point within the finite element model. ABAQUS solution dependent state variables, SDV2 and SDV6, are displayed in Figure 5 (a&b). State variable SDV2 represents the failure index at each integration point. It is a continuous variable that can have a value between 0 and 1. A value of 0 indicates there are no stresses at the integration point. A value of 1 indicates that the failure initiation criterion has been satisfied and the process of damage evolution (stiffness reduction) has begun at the integration point. Another useful state variable is SDV6, which is referred to as the damage variable D. SDV6 is a continuous variable with a value between 0 and 1 where a value of 0 corresponds to an undamaged integration point that has its original (full) stiffness, and a value of 1 corresponds to a fully degraded (zero stiffness) integration point. The FE analysed and the results were compared with experimental results.

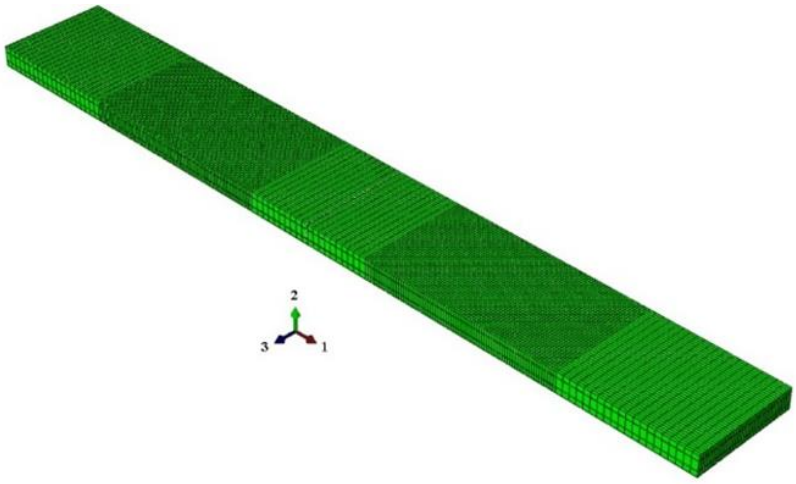

Figure 3. Three dimensional Finite element model of the delaminated specimen.

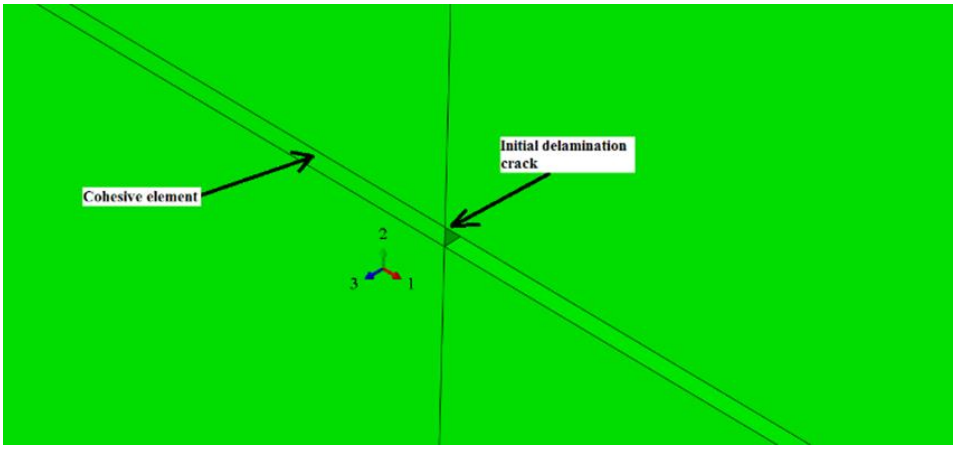

Figure 4. Cohesive element

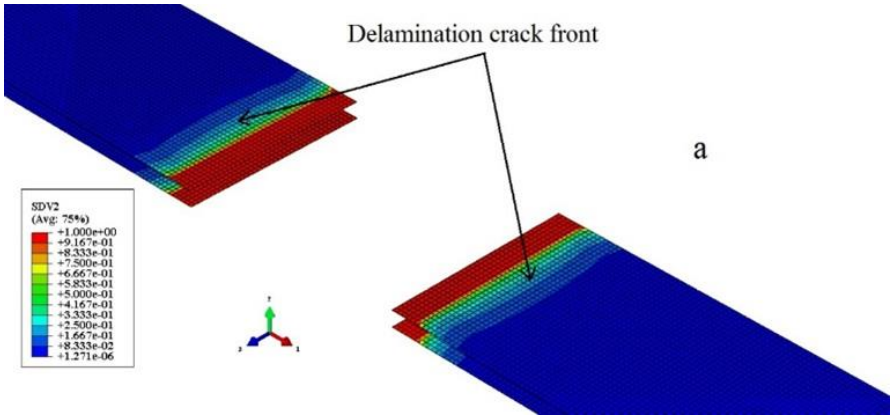

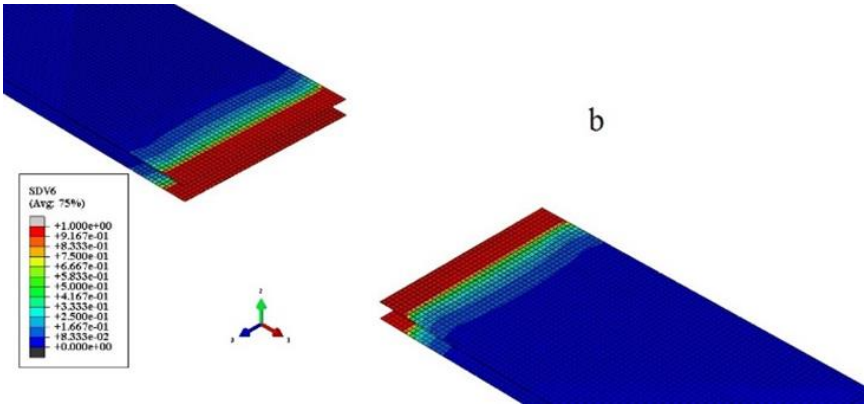

Figure 5. Damage in Cohesive element (Full model), (a) plot of the damage variable SDV2, (b) plot of the damage variable SDV6.

The propagation of delamination under increasing uniaxial load will generate stress concentration at the crack front, however it may not significantly alter the stress pattern on the outer surfaces. The stress concentration will be prominent if the crack surface is close enough to outer surface. The purposely created crack surface of the sample is relatively far from the top surface and a hole is drilled through the crack front (Figure6) of one of the specimen to see the prediction of DIC techniques for this study. Figure 7 shows the change of equivalent strain on the outer surface of the sample. Figure 8 shows strain map generated for the surface of specimen which has a similar delamination inside the sample under increasing tensile loading. Progression of the crack may have caused an increasing of strain field at the delaminated region. However, there is no significant strain concentration visible on the DIC strain map as anticipated.

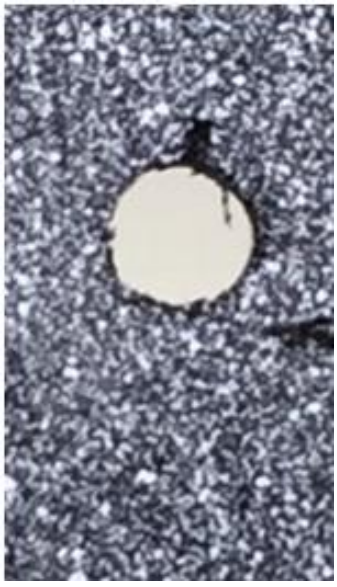

Figure 6. Holed composite specimen preparing for DIC test.

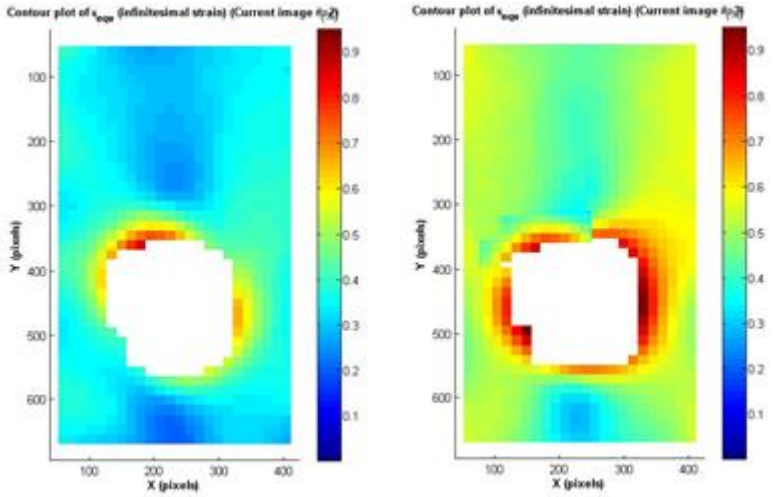

Figure7. Developing delamination damage from the hole which detecting use DIC technique.

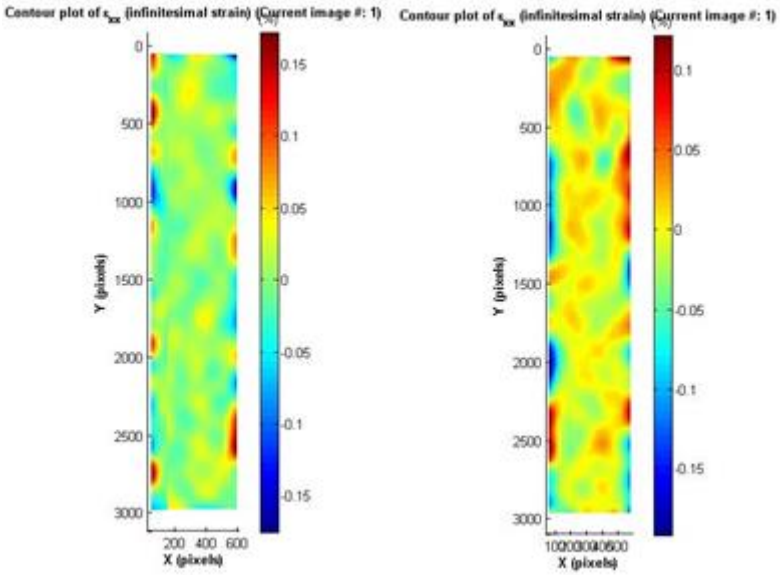

Figure 8. Detecting delamination damage use DIC technique at delamination region for embedded delamination composite specimen.

Figure 9 shows the thermoelastic phase response obtained through IR camera of the sample with purposely created delamination under cyclic loading. The variations in colour correspond to variation in the phase of the thermoelastic response relative to the applied cyclic load. The largest variations of phase are occurring near the bottom edge of the delamination zone. The original size of the delamination is approximately shown by the red dotted line in frame. This area is located within the area of perturbed phase response (defined by green hues) at the lowest mean load of 5 kN (0.11% strain). With the increase of mean load the perturbed area grows, and reaches a maximum at the mean load of 20 kN (0.66 % strain). The agreement between the experimental and numerical results is generally in a good agreement, but the latter yields consistently higher estimates of the delamination length.

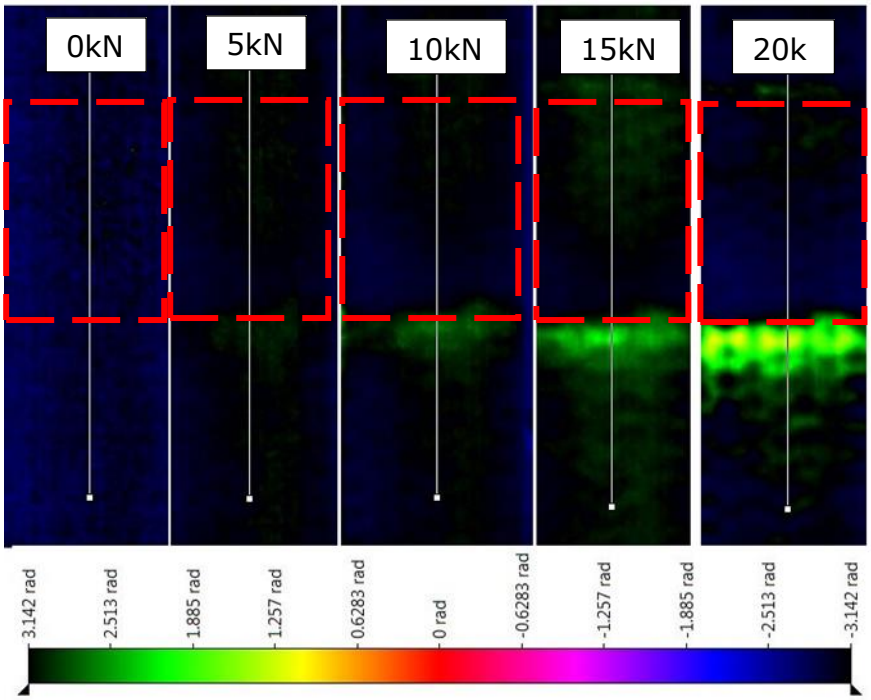

Figure 9. Delamination crack front propagation (θ-component). Red dotted line outlines the boundary of the initial delamination. Delamination zone is seen to increase as a function of mean load.

5. CONCLUSIONS

The delamination damage growth of a $[0/90]_{15}$ Woven Glass Fibre Reinforced Polymer Composite has been investigated experimentally and numerically. A monotonically increasing quasistatic load and a step-cyclic load regimes have been applied to a specimen with a purposely created delamination and its thermoelastic response was measured using a IR camera and DIC technique. The DIC technique has shown a potential of monitoring damage by strain mapping of outer surface of the sample. However, the location of the delamination through the thickness shown to be a governing factor of the sensitivity of DIC strain map. However, the TSA techniques have performed well for monitoring the delamination crack as anticipated.

An analysis of the delamination crack propagation on ABAQUS 6.13 has revealed that a cohesive element model provides reasonable accuracy for the simulation of damage growth in the class of specimen considered.

6. REFERENCES

1 R. Ambu, F. Aymerich, F. Ginesu, and P. Priolo, 'Assessment of Ndt Interferometric Techniques for Impact Damage Detection in Composite Laminates', *Composites Science and Technology,* 66 (2006), 199-205.

2 B. Pan, K. M. Qian, H. M. Xie , and A. Asundi, 'Two-Dimensional Digital Image Correlation for in-Plane Displacement and Strain Measurement: A Review', *Measurement science and Technology,* 20 (2009), 062001.

3 C. Colombo, L. Vergani, and M. Burman, 'Static and Fatigue Characterisation of New Basalt Fibre Reinforced Composites', *Composite Structures,* 94 (2012), 1165-74.

4 V. Crupi, E. Guglielmino, G. Risitano, and F. Tavilla, 'Experimental Analyses of Sfrp Material under Static and Fatigue Loading by Means of Thermographic and Dic Techniques', *Composites Part B: Engineering,* 77 (2015), 268-77.

5 Rami Haj-Ali, and Rani Elhajjar, 'An Infrared Thermoelastic Stress Analysis Investigation of Single Lap Shear Joints in Continuous and Woven Carbon/Fiber Epoxy Composites', *International Journal of Adhesion and Adhesives,* 48 (2014), 210-16.

6 Ayad Kakei, J. A. Epaarachchi, Mainul Islam, J. Leng, and N. Rajic, 'Detection and Characterisation of Delamination Damage Propagation in Woven Glass Fibre Reinforced Polymer Composite Using Thermoelastic Response Mapping', *Composite Structures,* 153 (2016), 442-50.

7 M. Kashtalyan, and C. Soutis, 'The Effect of Delaminations Induced by Transverse Cracks and Splits on Stiffness Properties of Composite Laminates', *Composites Part A: Applied Science and Manufacturing,* 31 (2000), 107-19.

8 S. Keshava Kumar, Ranjan Ganguli, and Dineshkumar Harursampath, 'Partial Delamination Modeling in Composite Beams Using a Finite Element Method', *Finite Elements in Analysis and Design,* 76 (2013), 1-12.

9 Behrad Koohbor, Silas Mallon, Addis Kidane, and Michael A. Sutton, 'A Dic-Based Study of in-Plane Mechanical Response and Fracture of Orthotropic Carbon Fiber Reinforced Composite', *Composites Part B: Engineering,* 66 (2014), 388-99.

10 P. F. Liu, and M. M. Islam, 'A Nonlinear Cohesive Model for Mixed-Mode Delamination of Composite Laminates', *Composite Structures,* 106 (2013), 47-56.

11 Abilash Nair, and Samit Roy, 'Modeling of Permeation and Damage in Graphite/Epoxy Laminates for Cryogenic Tanks in the Presence of Delaminations and Stitch Cracks', *Composites Science and Technology,* 67 (2007), 2592-605.

12 T. K. O'Brien, 'Characterization of Delamination Onset and Growth in a Composite Laminate', in *Damage in Composite Materials,* ed. by K. L Reifsnider (USA: ASTM STP 775. Am. Sot. Testing Marter., 1982), pp. 140-67.

13 Ramesh Talreja, and Chandra Veer Singh, *Damage and Failure of Composite Materials* (Unuited Kingdom: Cambridge, 2012).

14 J. L. Rebière, and D. Gamby, 'A Decomposition of the Strain Energy Release Rate Associated with the Initiation of Transverse Cracking, Longitudinal Cracking and Delamination in Cross-Ply Laminates', *Composite Structures,* 84 (2008), 186-97.

15 F. P. van der Meer, N. Moës, and L. J. Sluys, 'A Level Set Model for Delamination – Modeling Crack Growth without Cohesive Zone or Stress Singularity', *Engineering Fracture Mechanics,* 79 (2012), 191-212.